Chromophores

International Edition: DOI: 10.1002/anie.201410548
German Edition: DOI: 10.1002/ange.201410548

Excimers Beyond Pyrene: A Far-Red Optical Proximity Reporter and its Application to the Label-Free Detection of DNA**

Garam Han, Dongwook Kim, Younbong Park, Jean Bouffard, and Youngmi Kim**

Abstract: *A family of organic chromophores that, like pyrene, forms emissive excimers is reported. Their chemical and photophysical properties are superior to pyrene for the design of chemo- and biosensors. Unlike hydrophobic pyrene, which requires excitation by cell-damaging UV irradiation, these polar dyes absorb strongly in the visible range, and their excimers emit brightly in the red to far-red region of the electromagnetic spectrum. The intensity of the emission signal is greatly increased upon formation of a preassociated dimer that is triggered upon aggregation or crystallization. In demonstration of the potential of this new family of excimer-forming dyes, a probe that is capable of detecting label-free DNA in water down to 10 pM and also doubles as a visualization agent for DNA in gel electrophoresis is reported.*

The pyrene excimer is the classical example of excimer emission.[1] In dilute solutions ($\leq 10^{-5}$ mol L^{-1}) fluorescence emission from the pyrene monomer ($\lambda \approx 375$ nm) is detected upon UV irradiation; at increased concentrations ($\geq 10^{-3}$ mol L^{-1}) the red-shifted emission band of the excited pyrene face-to-face dimer appears ($\lambda \approx 480$ nm). Thanks to the predictability of this dual luminescence signal, pyrene moieties have been included in the design of numerous optical sensors as reporters of proximity. These include sensing schemes in which excimer emission signals the colocalization of sites of interest on a surface, such as that of lipid bilayers,[2] schemes in which aggregation or precipitation of a probe is triggered by an analyte,[3] or schemes in which analyte- or environment-dependent changes in the conformation of a biomolecule or a synthetic receptor bring tethered pyrenes into close proximity.[4]

These "turn-on" approaches in which a new signal arises with high sensitivity when molecules are brought into close proximity are inherently difficult to accomplish. Energy-transfer-based methods (e.g. fluorescence resonance energy transfer (FRET)) operate over larger distances, making them less sensitive tools to detect changes at close range (< 2–5 nm),[5] and most fluorescent dyes suffer from concentration quenching. The emission of the pyrene excimer remains by far the dominant proximity reporter, in spite of pyrene's punishing characteristics: its dismal aqueous solubility, limited synthetic tunability, excitation in the biomolecule-damaging UV region, and emission in the blue.[6,7]

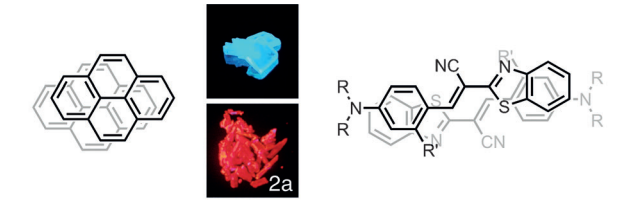

Pyrene Excimer:[1]
- λ_{max} (abs.)= 340 nm (UV)
- λ_{max} (em.)= 480 nm (blue)
- Crystal Packing: offset face-to-face dimers, 3.53 Å separation

Cyanovinylenes 1-3 Excimers (this work):
- λ_{max} (abs.)= 440-480 nm (tunable; blue)
- λ_{max} (em.)= 615-660 nm (tunable; red)
- Crystal packing: offset face-to-face dimers, 3.4-3.5 Å separation

The solid-state photophysical properties of cyanovinylene dyes **1a** and **2a** prompted us to investigate their potential for excimer emission. Whereas in dilute solutions these two cyanovinylene dyes emit weakly in the green (**1a**: $\lambda = 534$ nm, **2a**: $\lambda = 553$ nm), solid semicrystalline powders and single crystals exhibit a bright red luminescence (**1a**: $\lambda = 624$ nm, **2a**: $\lambda = 640$ nm; Figure 1 and Table 1). The red optical signature is also detected in highly concentrated solutions of **1a** in chloroform, a good solvent for this dye (see Figure S9 in the Supporting Information), indicating that aggregation or preassociation is not a prerequisite. These properties are unique to cyanovinylene derivatives of this family, as the vinylene analogues **1b** and **2b** do not exhibit this behavior. For the vast majority of fluorophores that show aggregation-induced enhanced emission (AIEE) or aggregation-induced emission (AIE), the uncharacteristic solid-state luminescence arises either from a rigidification that restricts non-radiative relaxation processes, the formation of molecular aggregates that favor exciton-coupled transitions (J aggrega-

[*] G. Han, Prof. Dr. Y. Kim
Department of Chemistry, Dankook University
126 Jukjeon-dong, Yongin-si, Gyeonggi-do 448-701 (Korea)
E-mail: youngmi@dankook.ac.kr
Prof. Dr. D. Kim
Department of Chemistry, Kyonggi University
154-52 Gwanggyosan-ro, Yeongtong-gu, Suwon 440-760 (Korea)
Prof. Dr. Y. Park
Department of Chemistry, Chungnam National University
220 Gung-dong, Yuseong-ku, Daejeon 305-764 (Korea)
Prof. Dr. J. Bouffard
Department of Chemistry and Nano Science (BK 21 Plus)
Ewha Womans University, 52 Ewhayeodae-gil
Seodaemun-gu, Seoul 120-750 (Korea)
E-mail: bouffard@ewha.ac.kr

[**] This research was supported by National Research Foundation (NRF) grants funded by the Korean government (2013M2B2A4041354 and 2012R1A1A2038694 for Y.M.K.; 2013R1A1A2011320 for J.B.). We thank Dr. Sang-woon Yoon for the deconvolution of absorption spectra, and Lucy Ping for comments and assistance with photography.

Supporting information for this article is available on the WWW under http://dx.doi.org/10.1002/anie.201410548.

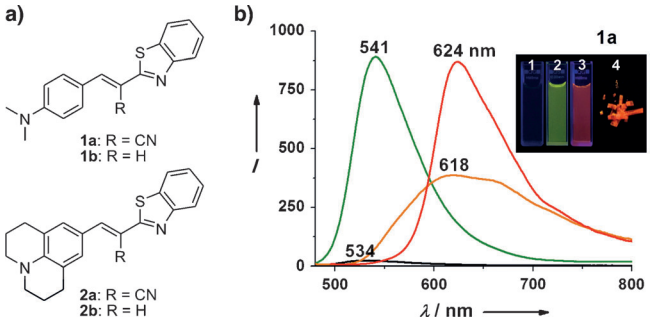

Figure 1. a) Structures of dyes **1**–**2** and b) emission spectra of **1a** (20 μM) in 1) CH_3CN solution (black line), 2) 10% methanol in glycerol (green line), 3) 10% CH_3CN in water (orange), and 4) as single crystals (red line). Excited at $\lambda = 440$ nm. Inset: photographs of the corresponding samples under irradiation with UV light at $\lambda = 365$ nm.

Table 1: Photophysical data for **1** and **2** in various media.

Compd.	λ_{abs} [nm][a] (log ε)	λ_{em} [nm][b] solution[c] (Φ_F)[d]	viscous media[e]	aggregates[f]	powdered solid[g]
1a	444 (4.89)	534 (0.001)	541	618	616 (624)
2a	479 (4.82)	553 (0.002)	563	659	650 (640)
1b	395 (4.73)	515 (0.014)	536	551	521
2b	418 (4.57)	541 (0.031)	561	565	561

[a] Absorption maximum measured in CH_3CN. [b] Emission maximum. [c] Measured in CH_3CN. [d] Quantum yields of fluorescence were determined using fluorescein ($\Phi_F = 0.95$) in NaOH (0.1 N) as standard. [e] Measured in 9:1 (v/v) glycerol:methanol containing DMSO (0.5%). [f] Measured in 9:1 (v/v) water:CH_3CN. [g] Values in parentheses are λ_{em} values for the single crystal. ε = molar extinction coefficient.

tion), or from polarity effects.[8] In the case of **1a** and **2a**, photophysical studies have established that these rationales are inoperative and that emission from an excited dimer is responsible for the new red-shifted emission.

Polarity effects were first ruled out by comparing emission in solvents with different dielectric constants (ε) ranging from toluene ($\varepsilon = 2.38$) to dimethyl sulfoxide ($\varepsilon = 47.2$). Although the emission maximum of **1a** and **2a** is slightly red-shifted in more polar solvents, the characteristic red-shifted emission band observed in the solid state is not detected (Table S1). Rigidification alone may also be excluded as the source of the new red-shifted emission band (Figures S3–S5). In a viscous glycerol solution or in a frozen methanol glass, the quantum yields (Φ_F) of **1a** and **2a** are increased as nonradiative deactivation pathways are restricted.[9] Nevertheless, the positions of the emission maxima remain unchanged compared to fluid solutions.

Aggregation of **1a** and **2a** can be triggered by the addition of water, a poor solvent, to acetonitrile solutions of the dyes. Increased proportions of water have little effect on the spectroscopic properties of **1a** and **2a** beyond that of medium polarity, until a solubility threshold is reached at an approximate $CH_3CN:H_2O$ ratio of 3:7 v/v. At this point, new spectroscopic features similar to those detected in the solid state arise: a) new, broad and significantly bathochromically shifted emission bands appear at $\lambda =$ 618 nm (**1a**) and 659 nm (**2a**); b) the fluorescence emission intensity is greatly increased at and above this threshold, with 74-fold and 55-fold respective increases for **1a** and **2a** (Figure 2). Dynamic light scattering (DLS) measurements confirm that the new spectroscopic features coincide with the formation of suspended molecular aggregates (Table S3). The aggregation behavior is replicated for **1a** and **2a** in solid poly(methyl methacrylate) solutions, where the prominence of the red-shifted AIE band increases slowly, until a concentration threshold is reached upon which growth of the AIE band accelerates rapidly to finally dominate the emission spectra (Figure S8). UV/Vis absorption spectra of the suspended aggregates are characteristic of chromophore interactions.[10] Deconvolution of the split absorption bands shows a shift to higher energy for **1a**, consistent with H-type aggregation. On the contrary for **2a**, a shift to lower energy is consistent with J-type aggregation. This discrepancy establishes that the new red-shifted emission

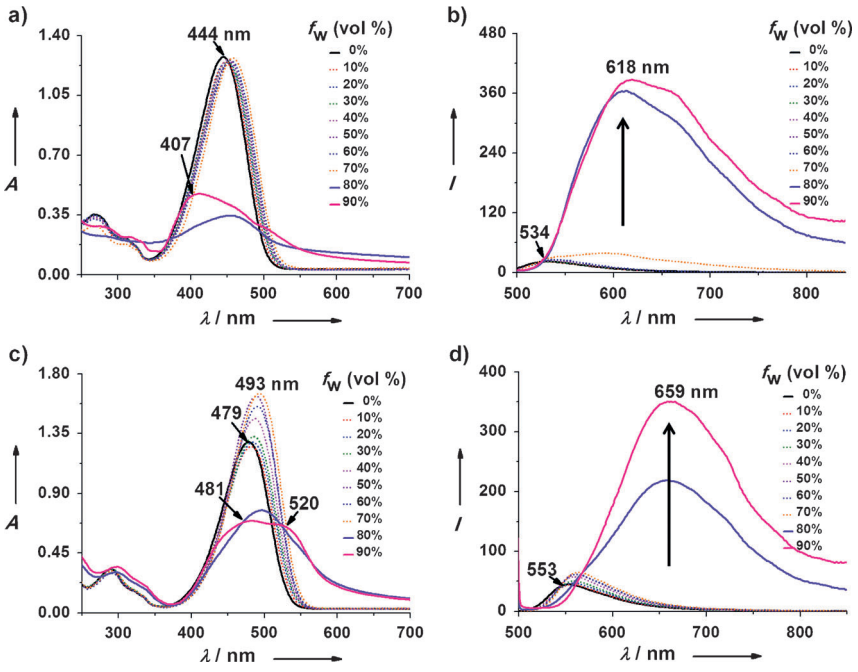

Figure 2. a, c) UV/Vis absorption and b, d) emission spectra of **1a** (a, b) and **2a** (c, d) in acetonitrile–water mixtures with different water fractions (f_w). [**1a**] = [**2a**] = 20 μM. $\lambda_{exc} = 440$ nm (**1a**), $\lambda_{exc} = 480$ nm (**2a**).

band seen for both **1a** and **2a** is not a result of exciton coupling between the chromophores (Figure S20).

The details of the molecular conformation and packing structure were obtained by single-crystal X-ray diffraction study.[11] Compounds **1a** and **2a** are nearly planar in the crystal, and arrange into offset columnar stacks of antiparallel dimers with close intermolecular stacking distances (3.48 Å for **1a** and 3.37 Å for **2a**; Figure 3). Given that the transition

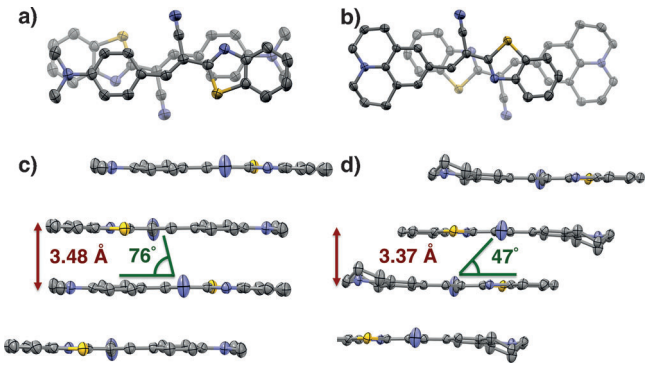

Figure 3. X-ray crystal structures of **1a** and **2a** drawn with thermal ellipsoids set at 50% probability and with hydrogen atoms omitted for clarity. a, b) Top view of the two nearest neighbor molecules in the crystal of **1a** (a) and **2a** (b). The molecules of **1a** (c) and **2a** (d) stack in offset columns of antiparallel dimers with displacement angles between nearest neighbors of 76° for **1a** and 47° for **2a**. Atom colors: C = gray; N = blue; S = yellow.

dipole in dyes **1a** and **2a** rests along the long molecular axis, the band splittings and blue or red shifts that arise in the UV/Vis absorption spectra of **1a** and **2a** upon formation of aggregates are consistent with the observed stacking angles.[10,12] The features present in the emission spectra of single crystals of **1a** and **2a** can be directly correlated with the packing structure determined by X-ray diffraction. AIE features are detected prominently in the single crystals, with strongly emissive broad bands centered at $\lambda = 624$ nm (**1a**) and 640 nm (**2a**), respectively. Since the new bands appear under either a H-type (**1a**) or a J-type packing (**2a**), these results also rule out exciton coupling as the origin of the new red-shifted emission band.

The excimer-like nature of the solid-state emission was finally established from the fluorescence lifetime of dyes **1**–**2** in varying media (Table 2). In dilute CH_3CN solution, where emission strictly occurs from the monomeric dyes, the decay of the excited states of **1a** and **2a** is single exponential with a short lifetime ($\tau_{1a} < 0.1$ ns, $\tau_{2a} = 0.29$ ns). In contrast, the excited-state decay dynamics of **1a** and **2a** in both the crystal and in semicrystalline powders are longer than those of solution ($\tau = 1$–5 ns) and are multiexponential in character. Moreover, suspended aggregates of **1a** and **2a** in CH_3CN–water mixtures (1:9, v/v) also show extended lifetimes ($\tau_{1a} =$ 0.92 ns; single exponential). The extended excited-state lifetimes that increase in prominence alongside increasing packing quality, and the offset π-stacked arrangement exhibited in the crystal, are entirely consistent with preassociated excimer emission being the origin of the new red-shifted

Table 2: Fluorescence decay of **1a** and **2a** in CH_3CN, CH_3CN–water mixture (1:9, v/v), and in the solid state.

Compd.	[a]	λ_{em} [nm]	τ_1 (f_1)[b] [ns]	τ_2 (f_2)[b] [ns]	τ_{avg}[c] [ns]
1a	A	520	< 0.1 (1)		< 0.1
	B	630	0.92 (1)		0.92
	C	630	1.61 (0.42)	5.04 (0.58)	4.38
	D	630	2.42 (0.28)	5.41 (0.72)	4.98
2a	A	550	0.29 (1)		0.29
	B	650	0.42 (0.77)	2.25 (0.23)	1.54
	C	650	1.42 (0.59)	3.36 (0.41)	2.63
	D	650	1.32 (0.64)	3.87 (0.36)	2.91

[a] Measured in A) CH_3CN solution; B) suspended aggregates in CH_3CN:water (1:9, v/v); C) semicrystalline powder; D) single crystal. [b] Lifetime (τ) and fraction (f) of shorter (1) or longer (2) lived species. [c] Weighted mean lifetime.

emission. In this regard, these features mirror those found for the excimer emission of pyrene in the solid state.[1] Herein for **1a** and **2a**, we employ Winnik's terminology of a preassociated excimer, also akin to a static excimer as opposed to a dynamic excimer as—just as for pyrene in the solid state—the chromophores also interact in the ground state, albeit to a limited degree. Such interactions should be absent in a genuine dynamic excimer according to the classical definition in which the ground state must be dissociated instead of only dissociative;[1] this situation prevails in concentrated solutions of these dyes in good solvents (Figure S9). Quantum chemical calculation results demonstrate that, despite the dark nature of their S_1 state, π-stacked dimers of **1a** can emit light from the S_2 state, which would be responsible for the excimer-like emission (Figures S39–S42). Given that both of these states are lower in energy by approximately 0.5–0.6 eV than the S_1 state of the monomer, and that the energy offset between them is as small as circa 70 meV, it is highly probable for **1a** dimers to be thermally activated to the S_2 state and to fluoresce bathochromically therefrom, which is also consistent with the rather long lifetime of the fluorescence of the **1a** crystal.

In this context, other examples relevant to our work must be mentioned. A first example is the observation by Weder et al.,[13] following earlier results by Hadziioannou et al.,[14] of a strong tendency toward excimer formation in crystalline solid cyano-substituted oligo(*p*-phenylene vinylene) derivatives. This tendency is facilitated by pronounced π–π interactions of planarized molecules stacked in a cofacial arrangement. Gierschner, Bazan, and co-workers also reported that for fluorinated distyrylbenzenes, cofacial π stacks of slightly offset chromophores resulted in a structureless and strongly red-shifted excimer-like emission analogous to that found for **1a** and **2a**.[15] Similar observations were reported by Würthner et al. for H aggregates of merocyanine dyes.[16] The recent work of Gierschner and Park on the photophysics of cyanodistyrylbenzenes that exhibit AIEE is also illustrative.[8g] Their observations highlight the importance of the cyanovinyl group to achieve tight packing arrangements in which the probability of nonradiative deactivation is significantly decreased.

We propose that **1a** and **2a**, which are readily excited by visible light and show excimer emission when brought in close

proximity or upon induced aggregation, could advantageously replace pyrene and its derivatives in sensing applications. Probes based on **1a** and **2a** further benefit from large Stokes shifts, which limit interferences due to the scattering of incident light, and from emission in the far-red region of the spectrum ($\lambda = 615$–660 nm). The emission overlaps with the near-IR (NIR) window of biological tissue transparency ($\lambda \approx 630$–900 nm) and is in a region largely devoid of autofluorescence, obviating the need for fluorescence lifetime discrimination techniques to filter out undesired signals.[4a,5a,17]

To demonstrate the potential of dyes related to **1a** and **2a** in biological sensing applications, we prepared the AIE-active cationic dye **3** and established its utility as a probe for the label-free detection of DNA (Figure 4). Unlike intercalating

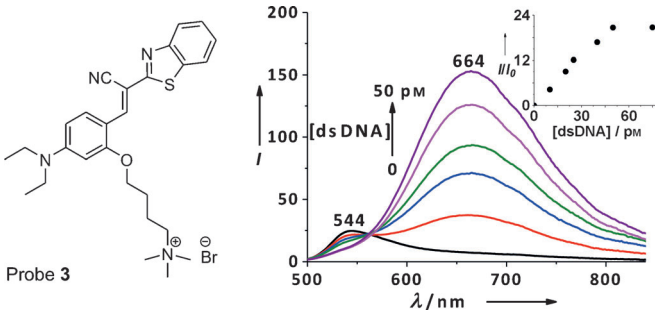

Figure 4. Emission spectra of probe **3** (20 μM) in the presence of different concentrations of dsDNA in HEPES buffer solution (10 mM, pH 7.4) at 25 °C. Inset: the relative fluorescence intensities of probe **3** monitored at λ = 664 nm upon addition of dsDNA. $\lambda_{exc} = 470$ nm.

dyes, probe **3** aggregates upon multivalent interactions with negatively charged biomolecules, resulting in an intense "turn-on" excimer emission signal.[3b,18] The UV/Vis absorption and emission spectra of **3** in aqueous buffer solution (10 mM HEPES, pH 7.4; HEPES = 2-[4-(2-hydroxyethyl)-1-piperazinyl]-ethanesulfonic acid) showed an absorption maximum at $\lambda = 466$ nm ($\varepsilon = 44\,200\ M^{-1}cm^{-1}$) and an emission maximum at $\lambda = 544$ nm with a small quantum yield of fluorescence ($\Phi_F \approx 0.005$). Upon addition of double-stranded (ds) calf-thymus DNA, a new structureless excimeric band centered at $\lambda = 664$ nm appears in the emission spectra, shifted 120 nm to the red of that of the free probe **3**. The fluorescence intensity of this new signal (I/I_o at $\lambda = 664$ nm) increases linearly with the concentration of dsDNA until saturation is reached at approximately 50 pM (or 0.43 ng μL^{-1}), where the intensity of the fluorescence signal has been enhanced 21-fold. Probe **3** also responds to single-stranded DNA (ssDNA), albeit with a lower sensitivity than for dsDNA (Figures S44–S45). Concomitantly with the rise of the new emission band, hypsochromic shifts are seen in the absorption spectrum that parallel those detected for the aggregated parent dye **1a**, and are consistent with the formation of H-type aggregates of **3** upon addition of nucleic acids (Figure S43). For biological applications, the characteristics of this "turn-on" excimer emission, as seen for **1a** and **2a**, compare advantageously to most reported dyes exhibiting

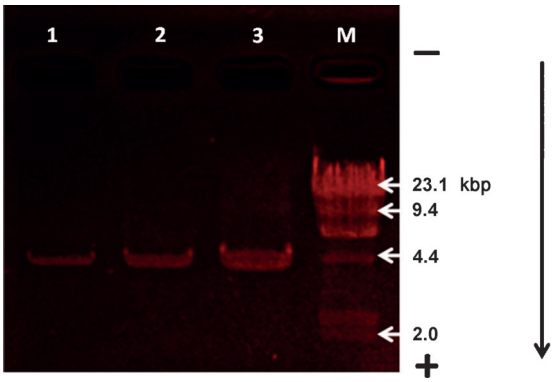

Figure 5. Image of agarose gel electrophoresis assays of plasmid DNA (4.1 kbp). Lanes 1, 2, and 3 were loaded with 64 μg, 128 μg, and 320 μg of DNA, respectively. Lane M: DNA molecular-weight marker. The gel was poststained by probe **3** (50 μM) for 60 min. The arrow indicates the direction of DNA migration.

AIE behavior, which are emissive in the blue or green regions of the visible spectrum.[8]

Probe **3** can be used not only for the detection of DNA in aqueous buffer solutions, but also as a staining agent for the gel electrophoresis of DNA (Figure 5). Plasmid DNA was electrophoretically separated on agarose gel before staining with a solution of probe **3** and rinsing with water, to reveal a gel showing red emission bands indicating electrophoretic DNA migration.

Cyanostilbenes **1a** and **2a** form red-emissive excimers. Although excimer emission is not particularly rare, no systems apart from that of pyrene itself have so far proved to be as usable and reliable in sensor design. The current work establishes the predictability and reliability of excimer emission from this family of dyes with the proof-of-concept water-soluble probe **3**, which allows for the label-free detection of DNA down to 10 pM in aqueous solutions, and its visualization in gel-electrophoresis assays without requiring UV irradiation.[6] The design of sensors and optical transducers of proximity based on the excimer-forming structures shared by dyes **1a**, **2a**, and **3** offers significant advantages by comparison with pyrene-centered designs, namely their modular synthesis, large Stokes shift, absorption in the visible region, and emission in the far red. The development of these systems in our laboratories is forthcoming.

Keywords: aggregation · chromophores · DNA detection · excimers · fluorescence

How to cite: *Angew. Chem. Int. Ed.* **2015**, *54*, 3912–3916
Angew. Chem. **2015**, *127*, 3984–3988

[1] a) T. Förster, *Angew. Chem. Int. Ed. Engl.* **1969**, *8*, 333; *Angew. Chem.* **1969**, *81*, 364; b) J. B. Birks, *Photophysics of Aromatic Molecules*, Wiley, New York, **1970**; c) J. B. Birks, *Rep. Prog. Phys.* **1975**, *38*, 903; d) N. J. Turro, *Modern Molecular Photochemistry*, University Science Books, Sausalito, **1991**; e) F. M. Winnik, *Chem. Rev.* **1993**, *93*, 587.

[2] "Pyrene-Labelled Lipids as Fluorescent Probes in Studies on Biomembranes and Membrane Models": P. K. J. Kinnunen, A.

Koiv, P. Mustonen in *Fluorescence Spectroscopy* (Ed.: O. S. Wolfbeis), Springer, Berlin, **1993**, pp. 159 – 171.
[3] a) C. Yu, V. W.-W. Yam, *Chem. Commun.* **2009**, 1347; b) R. Zhang, D. Tang, P. Lu, X. Yang, D. Liao, Y. Zhang, M. Zhang, C. Yu, V. W.-W. Yam, *Org. Lett.* **2009**, *11*, 4302; c) Y.-J. Huang, W.-J. Ouyang, X. Wu, Z. Li, J. S. Fossey, T. D. James, Y.-B. Jiang, *J. Am. Chem. Soc.* **2013**, *135*, 1700.
[4] For reviews, see: a) A. A. Martí, S. Jockush, N. Stevens, J. Ju, N. J. Turro, *Acc. Chem. Res.* **2007**, *40*, 402; b) J. S. Kim, D. T. Quang, *Chem. Rev.* **2007**, *107*, 3780; c) S. Karuppannan, J.-C. Chambron, *Chem. Asian J.* **2011**, *6*, 964; d) M. E. Østergaard, P. J. Hrdlicka, *Chem. Soc. Rev.* **2011**, *40*, 5771; e) E. Manandhar, K. J. Wallace, *Inorg. Chim. Acta* **2012**, *381*, 15.
[5] a) P. Conlon, C. J. Yang, Y. Wu, Y. Chen, K. Martinez, Y. Kim, N. Stevens, A. A. Marti, S. Jockusch, N. J. Turro, W. Tan, *J. Am. Chem. Soc.* **2008**, *130*, 336; b) S. Chen, L. Wang, N. E. Fahmi, S. J. Benkovic, S. Hecht, *J. Am. Chem. Soc.* **2012**, *134*, 18883.
[6] a) N. F. Cariello, P. Keohavong, B. J. S. Sanderson, W. G. Thilly, *Nucleic Acids Res.* **1988**, *16*, 4157; b) D. Gründemann, E. Schömig, *BioTechniques* **1996**, *21*, 898; c) H. A. Daum, M. Seville, *Mod. Drug Discovery* **2002**, *5*, 18; d) R. P. Sinha, D.-P. Häder, *Photochem. Photobiol. Sci.* **2002**, *1*, 225.
[7] For examples of pyrene derivatives with bathochromically shifted absorption and emission to overcome some of these limitations, see: H. Maeda, T. Maeda, K. Mizuno, K. Fujimoto, H. Shimizu, M. Inouye, *Chem. Eur. J.* **2006**, *12*, 824, and references therein.
[8] For recent reviews, see: a) Y. Hong, J. W. Y. Lam, B. Z. Tang, *Chem. Commun.* **2009**, 4332; b) J. Wu, W. Liu, J. Ge, H. Zhang, P. Wang, *Chem. Soc. Rev.* **2011**, *40*, 3483; c) Y. Hong, J. W. Y. Lam, B. Z. Tang, *Chem. Soc. Rev.* **2011**, *40*, 5361; d) B.-K. An, J. Gierschner, S. Y. Park, *Acc. Chem. Res.* **2012**, *45*, 544; e) Y. Zhao, L. Zhu, *J. Mater. Chem. C* **2013**, *1*, 1059; f) D. Ding, K. Li, B. Liu, B. Z. Tang, *Acc. Chem. Res.* **2013**, *46*, 2441; g) J. Gierschner, S. Y. Park, *J. Mater. Chem. C* **2013**, *1*, 5818; h) S. Varughese, *J. Mater. Chem. C* **2014**, *2*, 3499; i) J. Mei, Y. Hong, J. W. Y. Lam, A. Qin, Y. Tang, B. Z. Tang, *Adv. Mater.* **2014**, *26*, 5429.
[9] a) D. Oelkrug, A. Tompert, J. Gierschner, H. J. Egelhaaf, M. Hanack, M. Hohloch, E. Steinhuber, *J. Phys. Chem. B* **1998**, *102*, 1902; b) Z. R. Grabowski, K. Rotkiewicz, W. Rettig, *Chem. Rev.* **2003**, *103*, 3899; c) M. A. Haidekker, E. A. Theodorakis, *Org. Biomol. Chem.* **2007**, *5*, 1669.
[10] M. Kasha, H. R. Rawls, M. A. El-Bayoumi, *Pure Appl. Chem.* **1965**, *11*, 371.
[11] CCDC-1015967 (**1a**) and 1015968 (**2a**) contain the supplementary crystallographic data for this paper. These data can be obtained free of charge from The Cambridge Crystallographic Data Centre via www.ccdc.cam.ac.uk/data_request/cif.
[12] For a discussion of the limitations of this model, see the discussion by Gierschner and Park in Ref. [8g].
[13] a) C. Löwe, C. Weder, *Adv. Mater.* **2002**, *14*, 1625; b) C. Löwe, C. Weder, *Synthesis* **2002**, 1185; c) B. R. Crenshaw, C. Weder, *Chem. Mater.* **2003**, *15*, 4717; d) B. R. Crenshaw, C. Weder, *Adv. Mater.* **2005**, *17*, 1471; e) J. Kunzelman, B. R. Crenshaw, C. Weder, *J. Mater. Chem.* **2007**, *17*, 2989; f) J. Kunzelman, M. Kinami, B. R. Crenshaw, J. D. Protasiewicz, C. Weder, *Adv. Mater.* **2008**, *20*, 119; g) J. Kunzelman, T. Chung, P. T. Mather, C. Weder, *J. Mater. Chem.* **2008**, *18*, 1082.
[14] a) P. F. van Hutten, V. V. Krasnikov, H.-J. Brouwer, G. Hadziioannou, *Chem. Phys.* **1999**, *241*, 139; b) P. F. van Hutten, V. V. Krasnikov, G. Hadziioannou, *Acc. Chem. Res.* **1999**, *32*, 257.
[15] a) M. L. Renak, G. P. Bartholomew, S. Wang, P. J. Ricatto, R. J. Lachicotte, G. C. Bazan, *J. Am. Chem. Soc.* **1999**, *121*, 7787; b) J. Gierschner, M. Ehni, H.-J. Egelhaaf, B. M. Medina, D. Beljonne, H. Benmansour, G. C. Bazan, *J. Chem. Phys.* **2005**, *123*, 144914.
[16] a) F. Würthner, S. Yao, T. Debaerdemaeker, R. Wortmann, *J. Am. Chem. Soc.* **2002**, *124*, 9431; b) U. Rösch, S. Yao, R. Wortmann, F. Würthner, *Angew. Chem. Int. Ed.* **2006**, *45*, 7026; *Angew. Chem.* **2006**, *118*, 7184.
[17] a) C. J. Yang, S. Jockusch, M. Vicens, N. J. Turro, W. Tan, *Proc. Natl. Acad. Sci. USA* **2005**, *102*, 17278; b) A. A. Marti, X. Li, S. Jockush, Z. Li, B. Raveendra, S. Kalachikov, J. J. Russo, I. Morozova, S. V. Puthanveettil, J. Ju, N. J. Turro, *Nucleic Acids Res.* **2006**, *34*, 3161.
[18] a) M. Wang, D. Zhang, G. Zhang, Y. Tang, S. Wang, D. Zhu, *Anal. Chem.* **2008**, *80*, 6443; b) Y. Hong, M. Häußler, J. W. Y. Lam, Z. Li, K. K. Sin, Y. Dong, H. Tong, J. Liu, A. Qin, R. Renneberg, B. Z. Tang, *Chem. Eur. J.* **2008**, *14*, 6428.

Received: October 29, 2014
Revised: December 12, 2014
Published online: February 4, 2015

